Atypical and classical memory B cells produce *Plasmodium falciparum* neutralizing antibodies

Matthias F. Muellenbeck,[1] Beatrix Ueberheide,[3] Borko Amulic,[2] Alexandra Epp,[1] David Fenyo,[4] Christian E. Busse,[1] Meral Esen,[5,6] Michael Theisen,[7,8] Benjamin Mordmüller,[5,6] and Hedda Wardemann[1]

[1]Max Planck Research Group Molecular Immunology and [2]Department of Cellular Microbiology, Max Planck Institute for Infection Biology, 10117 Berlin, Germany
[3]Proteomics Resource Center, Department of Biochemistry and Molecular Pharmacology, and [4]Laboratory of Computational Proteomics, Center for Health Informatics and Bioinformatics, New York University Langone Medical Center, New York, NY 10016
[5]Institut für Tropenmedizin, Universität Tübingen, 72074 Tübingen, Germany
[6]Centre de Recherches Médicales de Lambaréné, B.P. 118 Gabon
[7]Department of Clinical Biochemistry and Immunology, Statens Serum Institute, 2300 Copenhagen, Denmark
[8]Centre for Medical Parasitology at Department of International Health, Immunology, and Microbiology and Department of Infectious Diseases, Rigshospitalet, University of Copenhagen, 1356 Copenhagen, Denmark

Antibodies can protect from *Plasmodium falciparum* (*Pf*) infection and clinical malaria disease. However, in the absence of constant reexposure, serum immunoglobulin (Ig) levels rapidly decline and full protection from clinical symptoms is lost, suggesting that B cell memory is functionally impaired. We show at the single cell level that natural *Pf* infection induces the development of classical memory B cells (CM) and atypical memory B cells (AtM) that produce broadly neutralizing antibodies against blood stage *Pf* parasites. CM and AtM contribute to anti–*Pf* serum IgG production, but only AtM show signs of active antibody secretion. AtM and CM were also different in their IgG gene repertoire, suggesting that they develop from different precursors. The findings provide direct evidence that natural *Pf* infection leads to the development of protective memory B cell antibody responses and suggest that constant immune activation rather than impaired memory function leads to the accumulation of AtM in malaria. Understanding the memory B cell response to natural *Pf* infection may be key to the development of a malaria vaccine that induces long-lived protection.

CORRESPONDENCE
Hedda Wardemann:
wardemann@
mpiib-berlin.mpg.de

Abbreviations used: AtM, atypical memory B cells; CM, classical memory B cells; FcRL4, Fc-receptor-like-4; GLURP, glutamate-rich protein; iRBC, infected RBC; MSP3, merozoite surface protein 3; *Pf*, *Plasmodium falciparum*; RBC, red blood cell.

Malaria caused by *Plasmodium falciparum* (*Pf*) infection is a leading cause of morbidity and mortality primarily in children in sub-Saharan Africa (Murray et al., 2012). Protective immunity to control clinical disease caused by parasite growth in red blood cells (RBCs) takes years to develop and requires repeated infections (Garnham, 1949). Human serum IgG antibodies can protect from blood stage parasitemia and malaria symptoms as demonstrated by historic passive transfer studies (Cohen et al., 1961). However, in the absence of constant reexposure, serum Ig levels rapidly decline and protection from malaria wanes, suggesting that protective humoral memory is not efficiently formed or is functionally impaired (Struik and Riley, 2004; Dorfman et al., 2005; Langhorne et al., 2008). Indeed, repeated *Pf* infection is associated with the accumulation of circulating atypical memory B cells (AtM) that are characterized by expression of the inhibitory Fc-receptor-like-4 (FcRL4; Weiss et al., 2009,

2010, 2011). FcRL4-positive memory B cells have originally been described in tonsils of healthy individuals (Ehrhardt et al., 2005, 2008). Circulating FcRL4-positive AtM also present in chronic HIV infection, where they show signs of functional exhaustion and hyporesponsiveness after in vitro stimulation suggesting that their memory B cell function is impaired (Moir et al., 2008). The role of AtM in immunity to malaria is speculative and it is unclear whether AtM contribute to the production of protective serum antibodies in vivo. To address these questions, we performed a molecular and functional characterization of the anti–*Pf* classical memory B cells (CM) and AtM response in immune adult donors from a malaria endemic

The Rockefeller University Press $30.00
J. Exp. Med. 2013 Vol. 210 No. 2 389-399
www.jem.org/cgi/doi/10.1084/jem.20121970

389

area. By single cell antibody cloning and mass spectrometry we show that CM and AtM express *Pf*-neutralizing antibodies and contribute to serum IgG production in vivo.

RESULTS

Pf-reactive CM and AtM in malaria immune adults

To determine the molecular and functional antibody characteristics of anti-*Pf* memory B cells, we set out to generate a panel of recombinant monoclonal antibodies from circulating IgG–positive CM and AtM of three asymptomatic semi-immune adults (MP036, MP070, and MP071; Table S1). The individuals were selected from a cohort of 67 healthy subjects with neutralizing serum IgG activity against asexual blood stage parasites from a highly endemic area in Gabon (Fig. 1 A; Dal-Bianco et al., 2007). All donors presented with a high frequency of circulating CD27⁻CD21⁻ AtM that showed increased FcRL4 and CD19 expression as well as lower IgG surface expression compared with CM (Fig. 1, B and C).

The *Pf* genome is highly complex, and only a few antigens out of the >5,000 possible protein products have been

associated with humoral protection against asexual blood stage parasites (Gardner et al., 2002; Fowkes et al., 2010). We therefore focused our analysis on two *Pf* antigens, merozoite surface protein 3 (MSP3) and glutamate-rich protein (GLURP), that have been described to induce serum IgG responses that are associated with protection from clinical malaria (Meraldi et al., 2004; Singh et al., 2009; Fowkes et al., 2010). Specifically, we studied the anti-*Pf* IgG B cell response to the vaccine candidate GMZ2, a fusion protein of the immune-dominant GLURP R0 nonrepeat region that is expressed at all parasitic life cycle stages in the human host, and the conserved domain of MSP3 that is critically involved in RBC invasion (de Stricker et al., 2000; Rodríguez et al., 2005; Esen et al., 2009). All individuals, including the selected donors, had high titers of serum IgG antibodies against GMZ2, MSP3, and GLURP and showed GMZ2 reactivity in CM and AtM (Fig. 1, D–F; and not depicted). In summary, the selected donors showed representative anti-*Pf* serum IgG and memory B cell responses as well as high frequencies of circulating AtM.
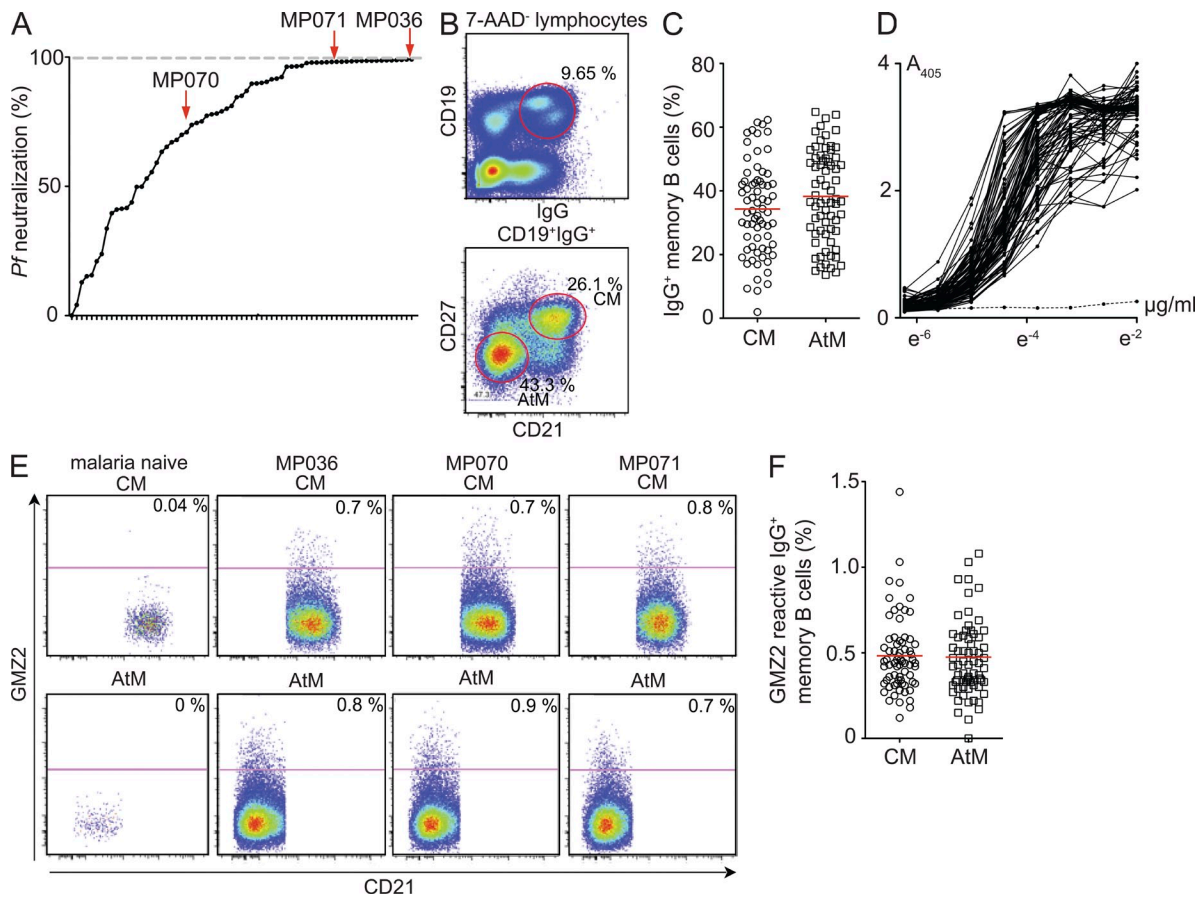

Figure 1. Memory B cell sorting. (A) Relative 3D7^Luc neutralizing activity of 100 µg/ml purified serum IgG from study participants in comparison to polyclonal serum IgG preparations from nonimmune controls (0% neutralization) and 50 mM chloroquine (100% neutralization, dashed gray line). Dots represent individual samples. Selected donors for antibody cloning are indicated. (B) Gating strategy for the flow cytometric isolation of CM and AtM. Representative plots from MP070 are shown. (C) Frequency of circulating CM and AtM. (D) IgG GMZ2 reactivity in serum as measured by ELISA. The dotted line shows a *Pf*-naive control serum. (E) Flow cytometric analysis of GMZ2-reactive CM and AtM in peripheral blood from MP036, MP070, and MP071 compared with a malaria naive donor. (F) Frequency of circulating GMZ2-reactive CM and AtM in all donors as determined in E. Red bars indicate arithmetic mean.

Ig gene repertoire of *Pf*–reactive CM and AtM

To generate recombinant monoclonal antibodies, the Ig gene variable regions of single isolated GMZ2-reactive CM and AtM from MP036, MP070, and MP071 were cloned into expression vectors (Tiller et al., 2008). Ig gene sequence analysis demonstrated that the memory IgG response was highly diverse (Tables S2–S4). No major differences in the *IGH* and *IGK* or *IGL* gene segment usage or *IGH* CDR3 features between CM and AtM were observed (Fig. 2, A–C; and Tables S2–S4). However, AtM had, on average, higher levels of somatic hypermutations in their V gene segments than CM (Fig. 2 D; mean ± SEM: AtM, *IGH* 28.1 ± 8.1, *IGK* 20.6 ± 9.1, and *IGL* 20.1 ± 1.7; CM, 24.5 ± 7.7, *IGK* 17.2 ± 9.5, and *IGL* 20.1 ± 1.5). *IGH* and *IGK/IGL* gene sequence alignments showed that clonally expanded B cells with identical Ig gene rearrangements were observed within both compartments. However clonally related CM and AtM were not detected in any of the three donors (Fig. 2 E). Statistical models based on the observed distributions of clonal relatives predict that if CM and AtM were directly derived from a shared ancestor, the likelihood of a random absence of shared clusters would be <0.1% on average for each of the donors. Thus, we conclude that CM and AtM show differences in their somatic hypermutation load and lack signs of clonal relationship, suggesting that the two populations may originate from different precursors.

Pf MSP3 and GLURP antigen specificity of CM and AtM antibodies

To determine whether anti-*Pf* CM and AtM show differences in their antigen reactivity, we expressed 236 recombinant monoclonal CM and AtM antibodies and performed ELISA (Fig. 3, A, C, and D; and Tables S2–S4). On average, 91 ± 7% of antibodies showed reactivity with the sort antigen GMZ2 (Fig. 3 A). For individual binders, reactivity with *Pf* merozoites was confirmed by fluorescence microscopy with infected RBCs (iR-BCs; Fig. 3 B). We further discriminated between MSP3 and GLURP antigen reactivity by ELISA (Fig. 3, C and D). MSP3-specific antibodies were more frequent than GLURP-specific antibodies in both memory B cell compartments (Fig. 3 E; mean ± SEM: MSP3, 70.3 ± 12.7% for CM and 67.3 ± 16.0% for AtM; GLURP, 17.0 ± 11.3% for CM and 11.3 ± 10.0% for AtM). However, even in the presence of high concentrations of
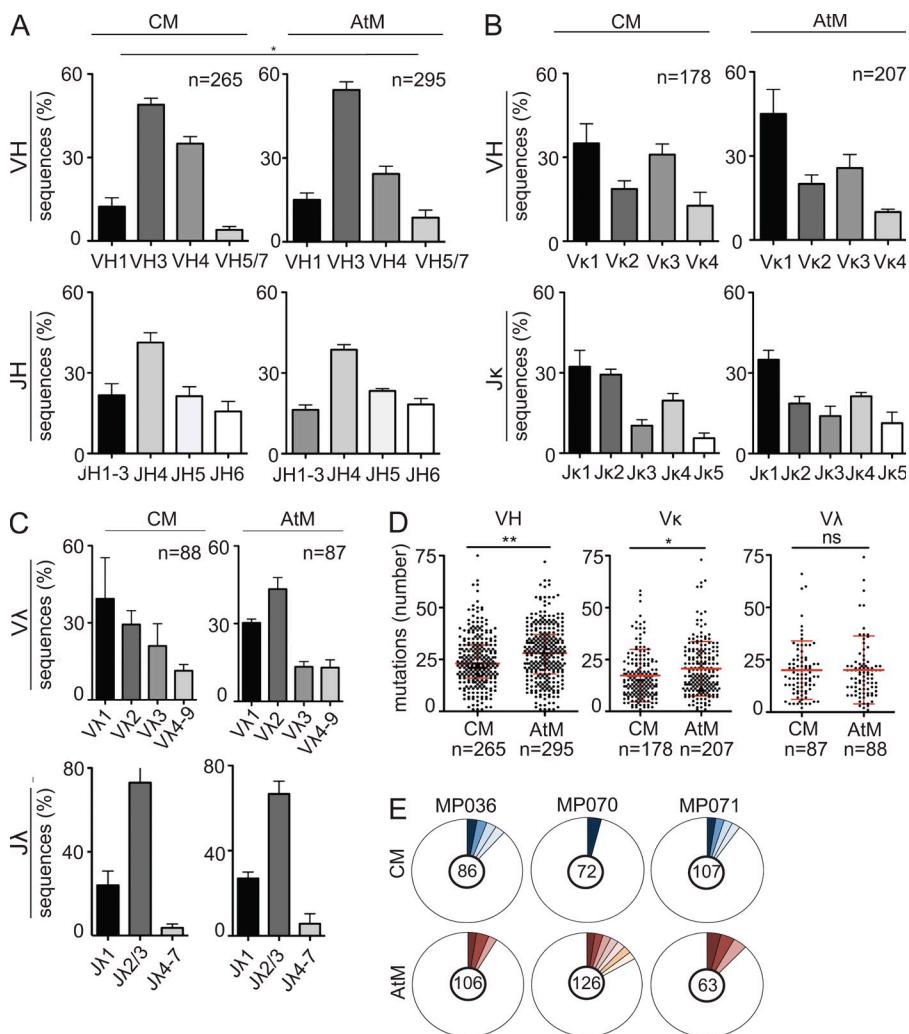

Figure 2. Antibody repertoire of CM and AtM. (A–C) *IGHV* and *IGHJ* (A), *IGLVK* and *IGLJK* (B), and *IGLVL* and *IGLJL* (C) gene family usage. The numbers of sequences analyzed are indicated. P-values were calculated using Fisher's exact test. (D) Absolute number of V segment somatic hypermutations. Geometric means with SD and the absolute numbers of sequences analyzed are indicated. P-values were determined using Student's *t* test. (E) Shaded pie areas indicate clonally expanded CM and AtM. Absolute numbers of sequences analyzed are indicated.
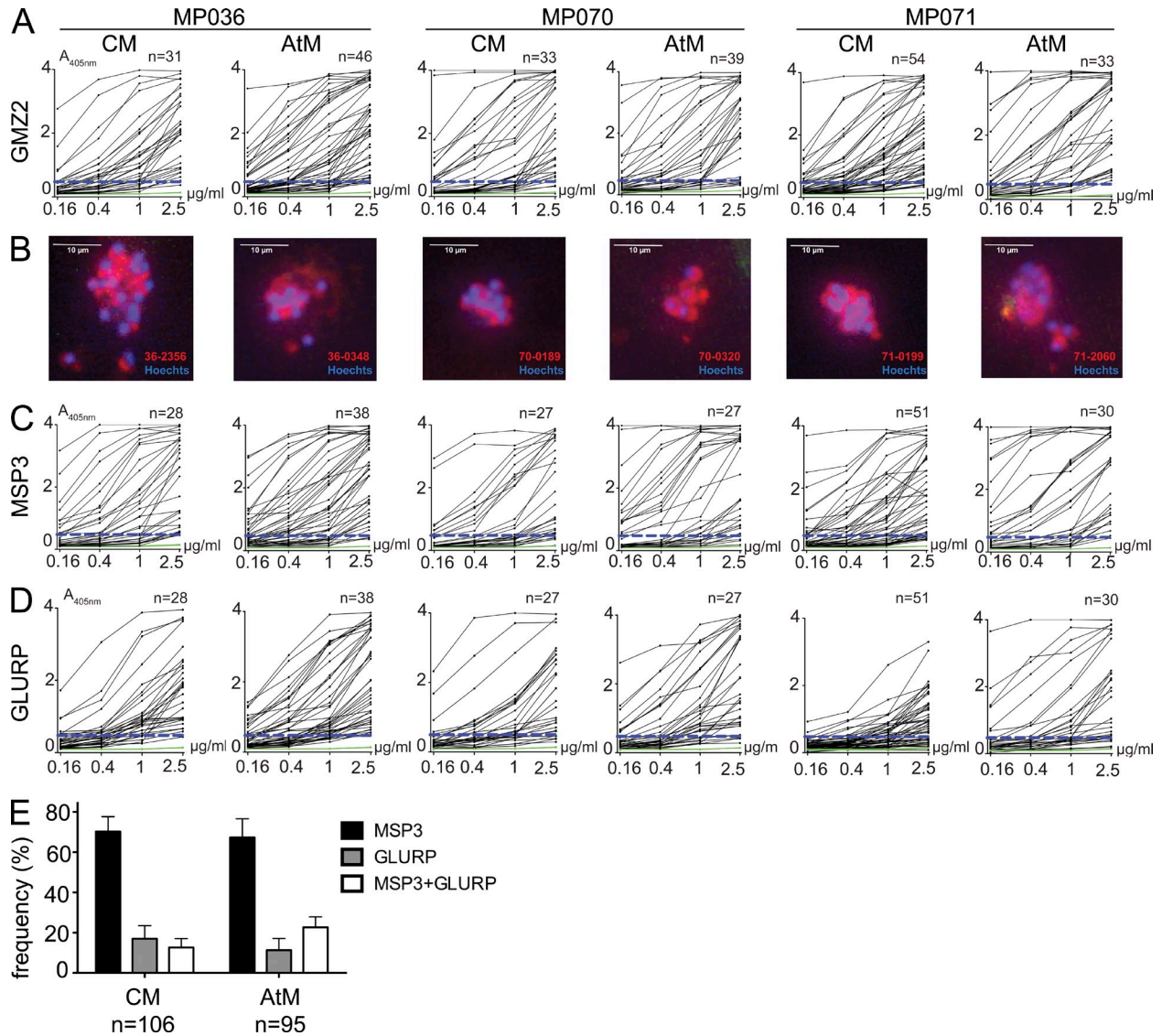
Figure 3. Anti–*Pf* CM and AtM antibody reactivity. (A) GMZ2 ELISA reactivity. The dashed blue line indicates the threshold OD$_{405nm}$ for positive reactivity. The green line represents the negative control antibody mGO53 (Wardemann et al., 2003). n indicates the numbers of tested antibodies. (B) Antibody reactivity (red) with *Pf* schizonts (blue) in iRBCs as measured by indirect immunofluorescence (bars, 10 μm). (C and D) ELISA reactivity of GMZ2-reactive antibodies (A) with MSP3 (C) and GLURP (D). (E) Bars summarize the mean frequency of MSP3, GLURP, and MSP3+GLURP reactive antibodies in all three donors (error bars indicate SEM).

BSA, ∼12.7 ± 7.7% of CM and 22.7 ± 9.0% of AtM antibodies bound both antigens at similar levels (Fig. 3 E and not depicted). In summary, the majority of GMZ2–reactive CM and AtM antibodies were MSP3 specific, but a fraction of the antibodies showed reactivity with GLURP or MSP3+GLURP.

Polyreactive antibodies are enriched in the anti–*Pf* AtM compartment
Dual reactivity with MSP3 and GLURP may suggest that the antibodies lacked *Pf* specificity and were polyreactive. To determine the degree of polyreactivity, we tested our collection of recombinant monoclonal antibodies for reactivity with diverse non–*Pf* antigens: bacterial LPS, human insulin, and double-stranded DNA (dsDNA; Fig. 4 A and Tables S2–S4).

The frequency of polyreactive antibodies was significantly higher in the AtM than in the CM compartment (Fig. 4 B; mean ± SEM: 64.3 ± 6.2% vs. 38.7 ± 8.4%; P = 0.004), and polyreactive antibodies were enriched in the MSP3+GLURP compartment (Fig. 4 C). However independently of the level of polyreactivity, anti–*Pf* antibodies, but not non–*Pf* reactive control antibodies, bound preferentially to iRBCs and not to non-iRBCs (Fig. 4 D). Thus, we conclude that CM and AtM express polyreactive and nonpolyreactive anti–*Pf* antibodies, and polyreactive antibodies are enriched in the AtM compartment.

CM and AtM antibodies neutralize *Pf* RBC invasion
Next, we tested if antibodies from *Pf*-reactive memory B cells neutralize asexual blood stage parasites (Fig. 5). Using an
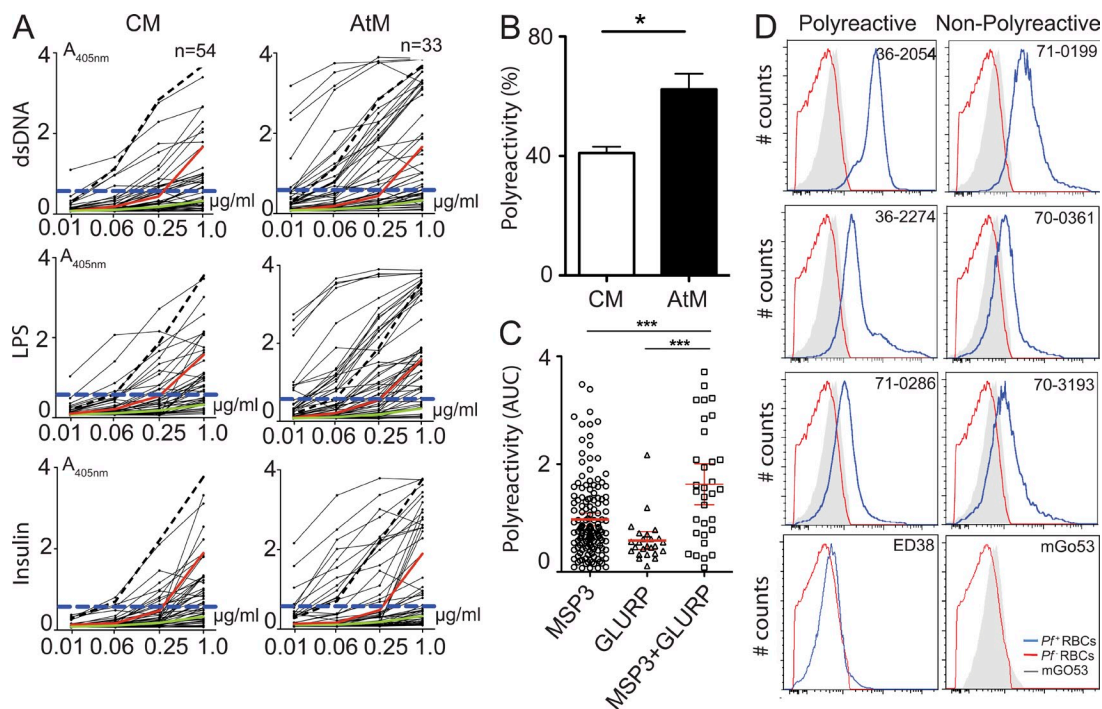
Figure 4. CM and AtM antibody polyreactivity. (A) ELISA reactivity with dsDNA, LPS, and insulin of CM and AtM antibodies from MP071. Non-polyreactive (green line; mGO53) and low (red line, JB40) and high (black dashed line, ED38) polyreactive control antibodies are shown. Dashed blue line indicates reactivity threshold. (B) Frequency of polyreactive CM and AtM antibodies from MP036, MP070, and MP071. (C) Symbols indicate antibody polyreactivity as the mean area under curve (AUC) for reactivity with dsDNA, insulin, and LPS. Horizontal lines indicate mean levels of antibody polyreactivity in all three donors. Error bars indicate SEM, and P-values were calculated using the ANOVA test. (D) Histograms show reactivity with noninfected Hoechst-negative RBCs (red line) and Hoechst-positive *Pf*-infected iRBCs (blue line) for representative polyreactive and nonpolyreactive anti-MSP3, anti-GLURP, and anti-MSP3+GLURP antibodies as determined by flow cytometry. Polyreactive (ED38) and nonpolyreactive (mGO53) control antibodies from malaria naive controls are shown. Gray areas show the iRBC reactivity of the non *Pf*-reactive isotype control antibody mGO53 in each plot. Data shown are representative for two independent experiments.

in vitro merozoite neutralization assay with genetically modified 3D7[Luc] *Pf* parasites expressing firefly luciferase, we measured the neutralization capacity at various antibody concentrations (Fig. 5 A; Lucumi et al., 2010). CM and AtM antibodies of all three donors showed various degrees of merozoite neutralization (Fig. 5 B). We conclude that the majority of IgG-positive GMZ2-reactive memory B cells express *Pf* inhibitory antibodies. Of note, we did not observe significant differences in the mean neutralization activity of CM and AtM antibodies or any correlation with MSP3 or GLURP antigen specificity or polyreactivity (Fig. 5 C). Although the MSP3 and GLURP antigens analyzed in this study are relatively conserved among different *Pf* strains and wild isolates, antigenic variation may limit the breadth of *Pf* neutralizing antibodies (Manske et al., 2012). To gauge the breadth of *Pf* inhibition, we tested a selected set of 25 3D7[Luc] neutralizing antibodies for neutralization of genetically diverse *Pf* isolates (DD2 [Thailand], IT2 [Brazil], and HB3 [Honduras]; Fig. 5 D and Tables S2–S4; Smilkstein et al., 2004; Johnson et al., 2007). The nontransgenic 3D7 strain was included for comparison. The antibodies were diverse in their neutralization efficacy and breadth, but individual antibodies showed comparable levels of neutralization for all strains, e.g., the CM antibodies 36–0003 and 71–2339 or the AtM antibody 71–0222

(Fig. 5 D). Thus, IgG memory B cells expressing neutralizing antibodies against genetically diverse asexual blood stage parasites develop in response to *Pf* infection.

CM and AtM contribute to the production of anti–*Pf* serum IgG

CM can contribute indirectly to the production of serum IgG antibodies after differentiation into antibody-secreting cells (Bernasconi et al., 2002), but whether AtM produce serum Ig in vivo is not known. To determine if the IgG antibodies that we cloned from CM and AtM could be detected in serum, we analyzed Fab2 fragments derived from protein G–purified MSP3- and GLURP-reactive serum IgG of donor MP036 by mass spectrometry (Fig. 6 A; Scheid et al., 2011). We then compared the amino acid sequences obtained from the mass spectrometric analysis to the Ig sequence database of the recombinant monoclonal CM and AtM antibodies from the same donor (Fig. 6 B and Fig. S1). We obtained amino acid sequence hits that mapped to the CM and AtM database but not to the international human protein index database, suggesting that both populations contribute to anti–*Pf* serum IgG production. By PCR, we were able to detect secretory IgG transcripts in AtM but not in CM, suggesting that AtM actively secrete antibodies in vivo and contribute directly to the humoral anti–*Pf* response (Fig. 6 C). Indeed, the IgG subclass
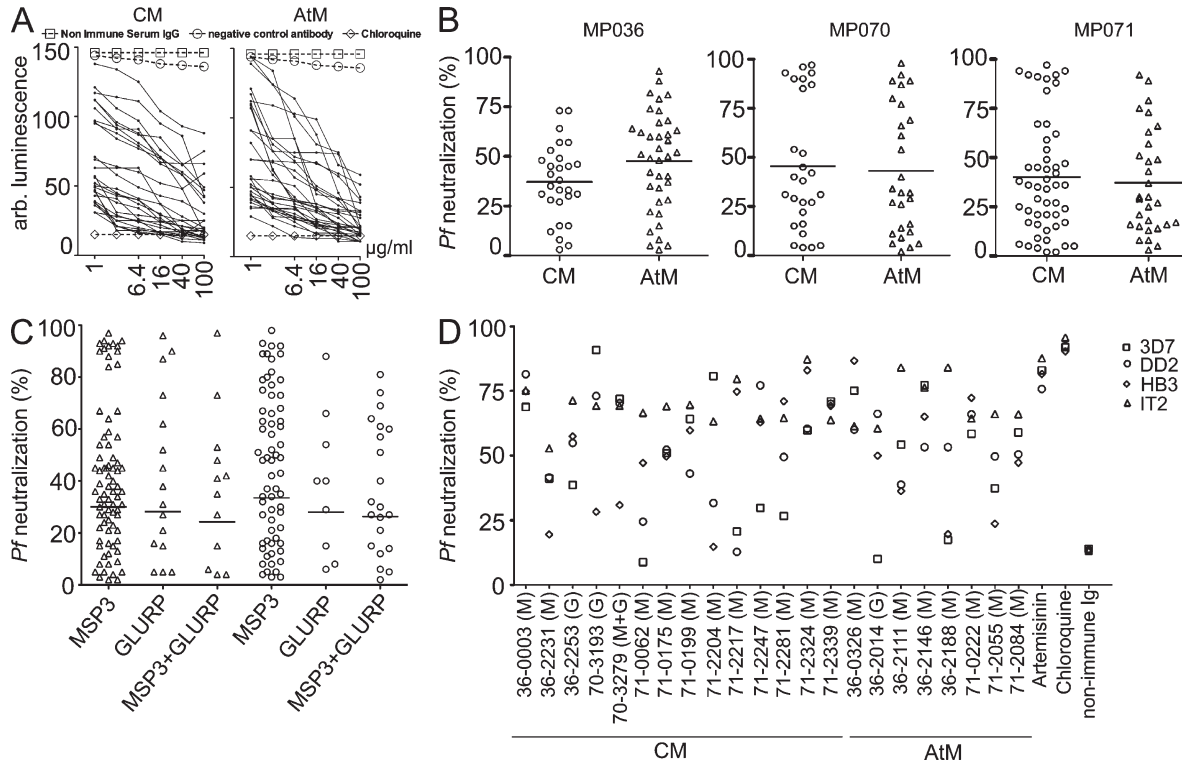
Figure 5. *Pf* merozoite neutralizing activity of CM and AtM antibodies. (A) 3D7^Luc transgenic parasite growth in the presence of individual antibodies (black lines; MP070) or the indicated controls. (B) Relative 3D7^Luc neutralizing activity of GMZ2-reactive antibodies at 6.4 µg/ml. Horizontal lines indicate mean neutralizing activity. (C) 3D7^Luc neutralizing activity of individual MSP3, GLURP, and polyreactive CM and AtM antibodies as in B. Black bars indicate geometric mean. (D) Relative *Pf* 3D7, HB3 (Honduras), DD2 (Thailand), and IT4 (Brazil) neutralizing activity of GMZ2-reactive antibodies at 100 µg/ml compared with chloroquine (100%). Parasites were detected using SYBR green. Data shown are representative of at least two independent experiments.

profile of AtM, but not of CM, was similar to the distribution observed for serum IgG antibodies (Fig. 6, D and E). Indicative of their activated and secreting phenotype, AtM showed higher CD19 and lower surface IgG and CD24 levels than CM, as well as increased surface expression of the activation markers HLA-DR, CD84, CD86, and CD319, but lacked the plasma cell marker CD138 (Fig. 7, A–I). Furthermore, AtM, but not CM, showed signs of proliferation as measured by flow cytometric DNA content measurements and Ki-67 expression level analysis (Fig. 7, J–L). We conclude that AtM and CM are functional and contribute directly and indirectly, respectively, to the production of *Pf*-inhibitory serum IgG antibodies.

DISCUSSION

In summary, we show that immunity to malaria is associated with the development of memory B cells that express *Pf* neutralizing antibodies and contribute to serum IgG production. In mice and humans, stable memory B cell responses against *Plasmodium* antigens have been detected, but whether the antibodies produced by memory B cells were neutralizing was not known (Wipasa et al., 2010; Nogaro et al., 2011; Ndungu et al., 2012). We found that the majority of memory B cell antibodies showed *Pf* neutralizing activity, including antibodies with broad neutralizing activity against genetically diverse *Pf* strains. Neutralization in our in vitro assays was a direct effect of antigen

reactivity, but in vivo Fc-mediated effector functions may add to parasite neutralization (Bouharoun-Tayoun et al., 1990).

Humoral immunity to MSP3 and GLURP has been associated with protection from malaria, and we observed neutralization for anti–MSP3 as well as anti–GLURP memory antibodies (Singh et al., 2009; Fowkes et al., 2010). Anti–MSP3 antibodies were more frequent than anti–GLURP antibodies, suggesting that MSP3 may be more efficient in inducing IgG memory B cell responses than GLURP. However, it cannot be excluded that the use of GMZ2 as bait for the isolation of anti–*Pf* memory B cells may enrich for MSP3-specific B cells. Differences in the nature of individual *Pf* antigens may account for differences in the induction of long-term humoral memory responses that have also been observed for viral and vaccine antigens (Taylor et al., 1996; Dorfman et al., 2005; Tongren et al., 2006; Amanna et al., 2007; Akpogheneta et al., 2008; Amanna and Slifka, 2010).

The relatively low level of antigenic variation in the MSP3 and GLURP peptides analyzed in this study may facilitate the generation of broadly inhibitory memory B cells (Manske et al., 2012). Whether neutralizing memory B cell antibodies are generated at similar frequencies to other antigens remains to be determined. Acquisition of protective humoral immunity to *Pf* may, however, also be associated with qualitative differences in the neutralizing activity of these antibodies. Thus, future studies
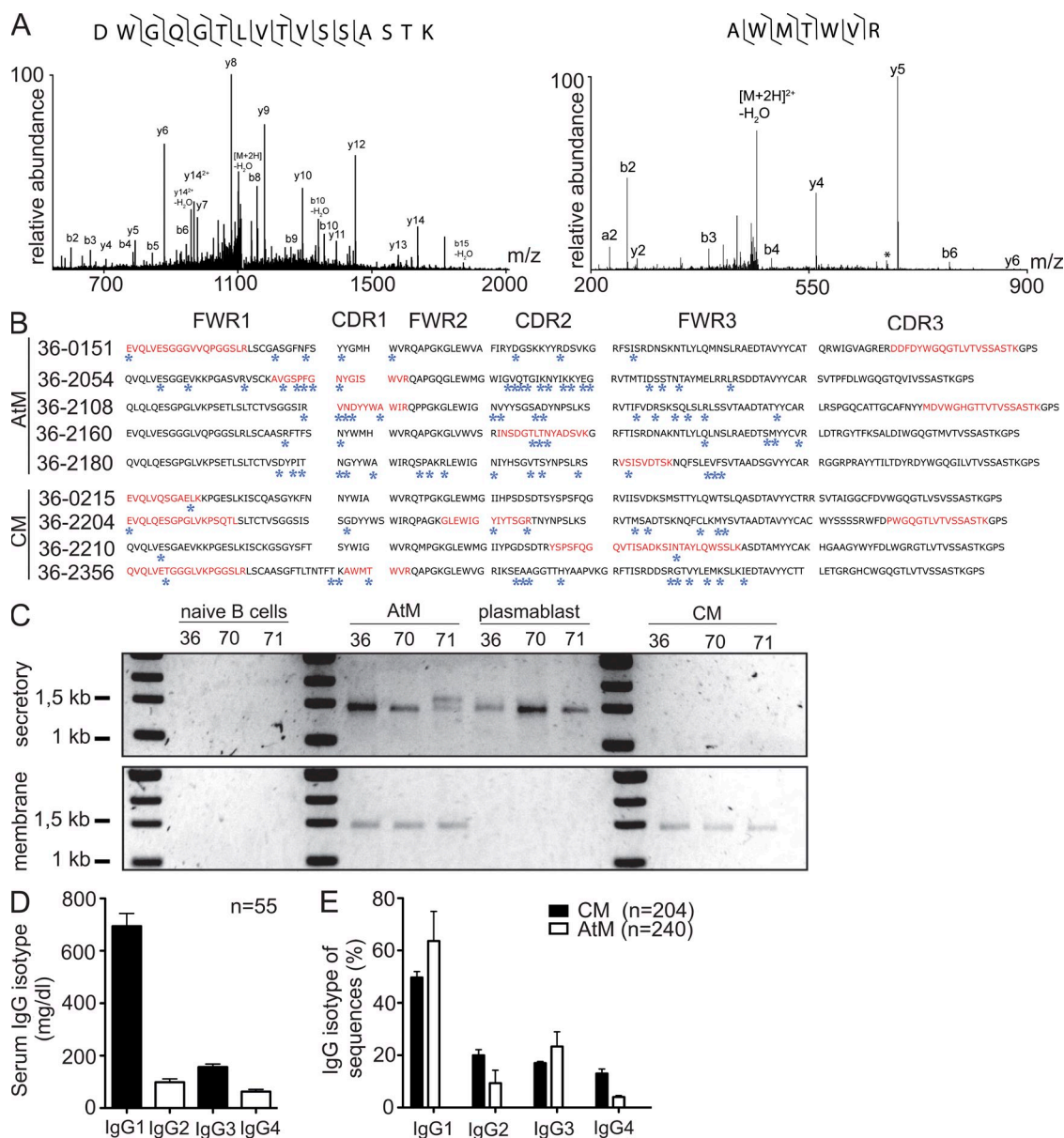
Figure 6. CM and AtM contribution to anti–*Pf* serum IgG. (A) Representative MS/MS spectra. Observed b-type fragment ions (containing the N terminus), y-type fragment ions (containing the C terminus), and loss of water (*) are indicated. Ions corresponding to the loss of water are labeled. Observed backbone cleavages are indicated (⌐ for b-type ions, ⌐ for y-type ions). Data shown are representative of at least three independent experiments on two different instruments. (B) IgH amino acid sequences of CM and AtM antibodies. Framework regions (FWR) and complementarity determining regions (CDR) are indicated. Blue stars indicate somatic point mutations. Mass spectrometric peptides with identical amino acid sequence are indicated in red. (C) RT-PCR amplicons of secretory and membrane IgG transcripts from the indicated B cell subpopulations. Data shown are representative of at least two independent experiments. (D) Serum IgG subclass distribution in donors from the Lambaréné area. (E) IgG subclass distribution as determined by *IGH* gene transcript sequence analysis. n indicates the number of tested sera. Error bars indicate SD.

will have to assess whether protection from clinical disease is not only associated with changes in the magnitude and overall breadth of the response but also with changes in the frequency of memory B cells that produce *Pf* neutralizing antibodies (Courtin et al., 2009; Nogaro et al., 2011). In addition, the role of IgM–expressing memory B cells in the response to *Pf* remains to be determined. Studies in mice suggest that long-term memory is predominantly the role of

IgM memory B cells, but their role in *Plasmodium* infection is not clear (Ndungu et al., 2009; Nduati et al., 2010; Reynaud et al., 2012). A thorough characterization of the quality and quantity of the human anti–*Pf* IgM memory B cell antibody response may help to elucidate the relative contribution of IgM versus IgG B cell memory to *Pf* in humans.

A large fraction of the recombinant monoclonal antibodies were polyreactive and such antibodies were enriched in the
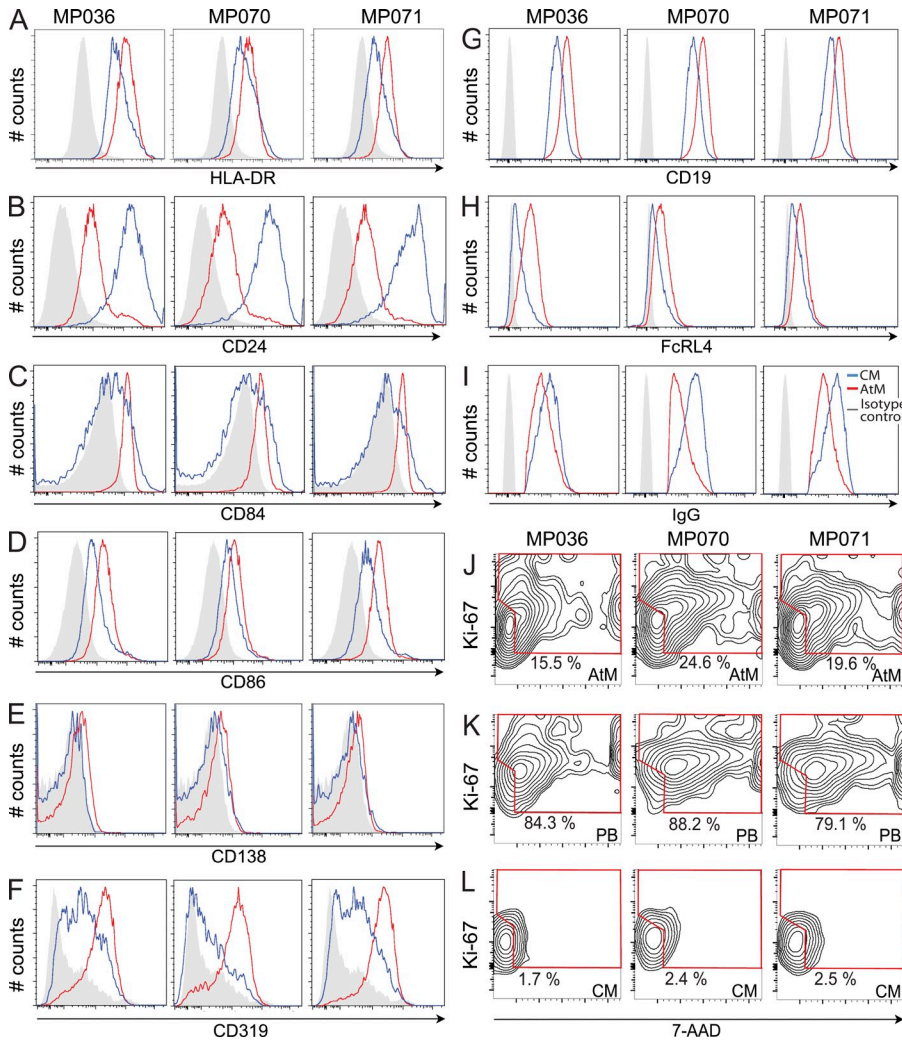
Figure 7. AtM express surface markers associated with B cell activation and show signs of recent cell divisions. Flow cytometric assessment of HLA-DR (A), CD24 (B), CD84 (C), CD86 (D), CD138 (E), CD319 (F), CD19 (G), FcRL4 (H), and surface IgG (I) surface expression levels on AtM (red line) and CM (blue line) from MP036, MP070, and MP071 in comparison to the isotype control (gray) are shown. Flow cytometric measurements of the DNA content and proliferation-associated Ki-67 protein expression levels in CD19+IgG+CD21−CD27− AtM (J), CD19+IgG+CD21−CD27+ circulating plasmablasts (PB; K), and CD19+IgG+CD21+CD27+CD38− CM (L) are also shown.

AtM compartment. However, polyreactive antibodies specifically recognized iRBCs and not non-iRBCs, suggesting that the level of binding to non-*Pf* antigens was relatively low compared with the affinity for *Pf*. Polyreactivity is a frequent feature of antibody responses to viral infections and has been shown to play a protective role against HIV, but whether such promiscuous antibodies are also beneficial in the immune response against *Pf* remains to be determined (Haynes et al., 2005; Mouquet et al., 2010; Mouquet and Nussenzweig, 2012).

AtM showed signs of activation, proliferation, and active antibody secretion, suggesting that their development in response to *Pf* is associated with differentiation into antibody-secreting cells rather than with a defect in B cell memory as previously proposed for HIV (Ehrhardt et al., 2008; Moir et al., 2010). Immunity to *Pf* is not sterilizing, and the frequent antigenic stimulation by repeated infections may induce *Pf*-reactive antigen-experienced B cells to develop into antibody-secreting cells and to acquire an AtM phenotype, a process which may be facilitated by the polyreactive nature of the antigen receptors expressed by AtM.

The relative contribution of AtM to the anti-*Pf* serum IgG response cannot be assessed, and although we demonstrate that

AtM secrete *Pf* neutralizing antibodies, it remains to be determined whether AtM fulfill true memory functions or if they simply represent a population of circulating short-lived antibody-secreting cells. The fact that AtM were almost negative for the plasma cell marker CD138, but showed signs of proliferative activity and expressed surface IgG as well as MHC II and various activation markers, supports the notion that AtM resemble plasma-blasts rather than long-lived plasma cells that were displaced from the bone marrow by recent infection (Ndungu et al., 2009).

The antibody repertoire of AtM was distinct from CM, suggesting that the two populations may develop from different precursors. A deeper analysis of the Ig gene repertoire of anti-*Pf* CM and AtM in comparison to tissue resident memory B cells and long-lived plasma cells may help to determine the origin of circulating AtM (Ehrhardt et al., 2005, 2008; Moir et al., 2008).

The memory B cell antibodies cloned in this study are fully human and may therefore be used in experimental human malaria infection to determine their protective efficacy against *Pf* asexual blood stages (Roestenberg et al., 2012). Understanding the protective properties as well as the limitations

in the memory B cell antibody response to *Pf* is crucial for developing vaccination strategies that elicit neutralizing antibodies to protect from clinical malaria.

MATERIALS AND METHODS

Study participants. Healthy adults (age 19–57 yr, mean 33 ± 10 yr) were recruited in the Lambaréné area (Gabon, Africa; Table S1). Peripheral blood samples were obtained after signed informed consent during dry season. None of the donors had previously participated in any malaria vaccine study. Parasitemia was assessed by microscopy, PCR (*stevor*), and rapid diagnostic test (NOW ICT Malaria Test; Binax Inc.). Ethical approval was obtained from the Comité d'Ethique Regional Independent de Lambaréné (No. 17/10).

Flow cytometry. Peripheral blood mononuclear cells were purified using Percoll gradient density centrifugation. Flow cytometric analyses were performed on an LSR II instrument (BD). IgG memory B cells were isolated using an ARIA II flow cytometric cell sorter (BD). *Pf* GLURP, MSP3, and GMZ2 antigens were produced and purified as previously described (Theisen et al., 2004). GMZ2 was chemically coupled to Alexa Fluor 647 according to the manufacturer's instructions (Life Technologies). For use in flow cytometry, the following mouse antibodies were used: anti–human CD19-PE-Cy7, anti–human IgG-APC-H7, anti–human CD27-FITC, anti–human CD38-V450, anti–human CD86-FITC, anti–human CD138-FITC (all from BD), anti–human CD21-PE, anti–human CD21-APC, anti–human CD24-biotin, anti–human CD27-biotin, anti–human CD84-biotin, anti–human HLA-DR-APC (all from eBioscience), anti–human Ki-67-PE (BioLegend), and anti–human FcRL4-biotin (gift of G.H. Ehrhardt and M. Cooper, Emory University School of Medicine Atlanta, GA). Streptavidin-QDot605 (Life Technologies) was used to detect biotin-conjugated primary antibodies. 7-AAD (Life Technologies) was used in all experiments to exclude dead cells. For intracellular stainings with anti–human Ki-67-PE (BioLegend) and 7-AAD (Invitrogen), PBMCs were permeabilized using Fix & Perm solution (BD) according to the manufacturer's instructions.

Single-cell sorting and antibody cloning. Single-cell sorting and antibody cloning was performed as previously described with the following modifications: cells were sorted into 384-well plates and volumes of RT-PCR reactions were scaled by a factor of 0.25 (Tiller et al., 2008; Scheid et al., 2011). In brief, single cells were isolated using flow cytometric cell sorting. cDNA was generated in the original 384-well sort plates. Ig gene transcripts were amplified by nested RT-PCR, and sequenced and cloned into IgG1 heavy and Igκ or Igλ light chain expression vectors, respectively. For in vitro antibody production, HEK293T cells were cotransfected with Ig heavy and matching Ig light chain plasmids. Recombinant monoclonal antibodies were purified from culture supernatant under sterile conditions using protein G beads. Antibodies were eluted from protein G beads using 0.1 M glycine, pH 3, and neutralized in 10× PBS for use in ELISA and neutralization assays. IgG concentrations were determined by ELISA.

ELISA. ELISAs were performed as previously described (Tiller et al., 2008). In brief, antigens or goat anti–human IgG (Dianova) were coated overnight at 4°C. For *Pf* antigen ELISAs, GMZ2, MSP3, or GLURP were coated at a concentration of 10 ng/well and plates were blocked with PBS-B (1× PBS, 0.005% vol/vol Tween-20, and 0.01% wt/vol EDTA) supplemented with 1% BSA for 1 h before incubation with recombinant monoclonal antibodies for 2 h at room temperature. For polyreactivity ELISAs, antigens were coated at with 10 µg/ml dsDNA or LPS or 5 µg/ml insulin and plates were blocked with PBS-B for 1 h. For IgG concentration ELISAs of purified serum IgG or recombinant monoclonal antibodies, human IgG1κ from plasma of myeloma patients (Sigma-Aldrich) was used as standard. Bound recombinant monoclonal antibodies were detected using anti–human IgG-HRP antibody (Dianova). Anti–human IgG-HRP antibodies were detected using one-step ABTS substrate (Roche). Area-under-curve (AUC) values were calculated using PRISM (GraphPad Software). Antibodies were considered polyreactive when they recognized at least two out of the three structurally different antigens: dsDNA, insulin, and LPS. Internal high (ED38) and low (JB40) positive and negative (mGO53) control antibodies were used in all assays to set thresholds for polyreactivity (Wardemann et al., 2003; Meffre et al., 2004; Tiller et al., 2008).

***Pf* cultures and inhibition assays.** Parasites were cultured under standard conditions. In brief, *Pf* clone 3D7 and isolates DD2, HB3, and IT2 were cultivated at 5% hematocrit in RPMI 1640 supplemented with 0.05 g/liter hypoxanthine (Sigma-Aldrich), 25 mM Hepes, 0.5% Albumax II (Life Technologies), 0.25% sodium bicarbonate, and 0.01 mg/ml gentamicin (Sigma-Aldrich). All cultures were kept at 37°C under 90% nitrogen, 5% oxygen, and 5% carbon dioxide. 3D7[Luc] cultures were supplemented with 40 ng/ml pyrimethamine to ensure transgene expression. Neutralization assays were performed with synchronized late stage 3D7[Luc] or 3D7, DD2, and HB3 cultures at a starting parasitemia of 0.2 or 0.5%, respectively. Parasites were cultured in duplicates in the presence of recombinant monoclonal antibodies or protein G purified serum IgG. Uninfected cultures, chemical inhibitors (chloroquine and artemisinin at 50 mM), whole serum (10%), and mGO53 (non-*Pf* reactive recombinant monoclonal antibody) were used as internal controls. 3D7[Luc] growth was measured after merozoite release and reinvasion after 24 h by quantifying luciferase activity using Bright-Glo Luciferase substrate (Promega). Arbitrary luminescence units were measured on a VICTOR light reader (1420 Luminescence Counter; PerkinElmer). Growth of 3D7, HB3, IT4, and DD2 cultures was assessed after 48 h using SYBR green (Smilkstein et al., 2004). Fluorescence was measured on a Fluoroskan Ascent reader (Thermo Fisher Scientific).

Indirect immunofluorescence assay. Late stage percoll-sorbitol purified *Pf* 3D7 iRBCs were allowed to settle on poly-L-lysine–coated glass slides. Cells were fixed with 4% paraformaldehyde/0.0075% glutaraldehyde before permeabilization with 0.2% Triton X-100. Blocking with BSA (3%) was performed before incubation with individual human recombinant monoclonal antibodies (10 µg/ml). Bound antibodies were detected using Cy3-conjugated mouse anti–human IgG-Fc (Jackson ImmunoResearch Laboratories). Hoechst 33342 was used to stain parasite DNA (Life Technologies). Images were acquired on a microscope (DMR; Leica) with an HCX PL FLUO-TAR 100×/1.3 objective using a digital camera (DXM 1200F; Nikon). ACT-1 (version 2.7; Nikon) was used as acquisition software.

Secretory and membrane IgG PCR. CM, AtM, naive B cells (CD19^{+}IgM^{+}IgD^{+}), and plasmablasts (CD19^{+}CD27^{+}CD38^{+}IgG^{+}) were bulk isolated by flow cytometric cell sorting. Secretory and membrane IgG transcripts were amplified by RT-PCR using an *IGHV* gene forward primer mix and 5′-TCCTCGCGCGACCCCGAGAGC-3′ (secretory) or 5′-GTC-CACAGCCCGTCCAGCTCCC-3′ (membrane) as reverse primer, respectively. Amplification was performed using HotStar Taq (QIAGEN) at 94°C for 15 min, 50× (94°C for 30 s, 68°C for 45 s, and 72°C for 30 s), 72°C for 10 min for secretory and 94°C for 15 min, 50× (94°C for 30 s, 65°C for 45 s, and 72°C for 2 min), and 72°C for 10 min for membrane IgG transcripts. PCR products were separated on 2% agarose gels.

Mass spectrometry. Mass spectrometric analyses were performed as previously described (Scheid et al., 2011). In brief, Fab2 fragments were generated from protein G–Sepharose purified serum IgG. MSP3 and GLURP reactive Fab2 fragments were isolated using HIS-tagged MSP3 and GLURP, respectively, and anti-HIS Dynabeads (Life Technology). MSP3 and GLURP reactive Fab2 fragments were reduced with dithiothreitol, alkylated using iodoacetamide, resolved by 1D gel electrophoresis on a 4–12% NuPAGE Novex Bis-Tris gel (Invitrogen), and stained with Coomassie Blue (Thermo Fisher Scientific). Fab2 fragments were excised from the gel and digested using 200 ng trypsin (Promega). The resulting peptides were isolated using reverse phase resin (PORS 20 R2; Applied Biosystems) and eluted using 40% acetonitrile in 0.5% acetic acid, followed by 80% acetonitrile in 0.5% acetic acid. Acetonitrile was removed using a speedvac (Thermo Fisher Scientific). The peptides were resuspended in 0.5% acetic acid and injected onto a Pico-Frit column (New Objective) with integrated emitter tip (360 µm O.D., 50 µm I.D., 10 µm tip), packed with 10 cm of reverse-phase ProteoPepII (New Objective) using a Proxeon nLC 1000 (Thermo Fisher Scientific). The HPLC column was interfaced to either an Orbitrap Velos or a Q Exactive Orbitrap mass spectrometer (Thermo Fisher Scientific). The peptides were eluted using the following gradient: 0–5% B in 5 min, 40% B in 125 min, 60% B in 150 min, 100% B in 165 min (A = 0.1 M acetic acid, B = 90% acetonitrile in

0.1 M acetic acid, flow rate 200 nl/min). Both instruments were operated in a data-dependent mode. For analysis on the Orbitrap Velos, a full scan was followed by a 20 MS/MS scans on the 20 most abundant ions in that full scan. The peptides (only charge states >1 and <5) were isolated with a 2D window, target window of $1e^4$ ions, dissociated via CAD (normalized collision energy = 35, activation Q = 0.25, activation time = 30 ms) and mass analyzed in the LTQ. For analysis on the Q Exactive Orbitrap, a full scan (resolution 70,000 at m/z 200) was followed by a 10 MS/MS scans on the 10 most abundant ions from the preceding full scan. The peptides (only charge states >1 and <5) were isolated with a 2D window, target window of $2e^5$ ions, dissociated with normalized collision energy of 27, and mass analyzed with a resolution of 17,500 (at m/z 200). For either instrument, the ions selected for MS/MS were set on an exclusion list for 30 s. The resulting MS/MS spectra were searched against the Human IPI and in-house-specific IgG database using Xtandem!. Peptide hits corresponding to GMZ2-reactive CM or AtM IgH sequences were manually confirmed.

SNP analysis and stochastical calculation. MSP3 (PF10_0345) and GLURP (PF10_0344) SNP analysis was performed using next-generation sequencing data of 222 *Pf* isolates supplied by the MalariaGen Genomic Epidemiology Network (Manske et al., 2012; Data Release 1.0).The mean number of clusters of clonally related cells was determined by maximum likelihood estimations using a multivariate hypergeometric distribution model and the singlet/doublet frequencies observed over all donors/populations while assuming a uniform size of the individual clusters. If CM and AtM cells differed in their surface phenotype but were derived from the same population, the likelihood of not observing any shared clusters within an individual donor can be approximated as $(1 - a/c)^b$, where c is the calculated overall number of clusters, a the number of unique clusters sampled from the first population, and b the number of unique samplings from the second population.

Online supplemental material. Fig. S1 provides peptide data for the mass spectrometric analysis of purified anti-GMZ2 serum IgG from MP036. Table S1 provides clinical information on blood samples from MP036, MP070, and MP071. Tables S2, S3, and S4 provide Ig gene and antibody reactivity information for antibodies from MP036, MP070, and MP071, respectively. Online supplemental material is available at http://www.jem.org/cgi/content/full/jem.20121970/DC1.

REFERENCES

Akpogheneta, O.J., N.O. Duah, K.K. Tetteh, S. Dunyo, D.E. Lanar, M. Pinder, and D.J. Conway. 2008. Duration of naturally acquired antibody responses to blood-stage *Plasmodium falciparum* is age dependent and antigen specific. *Infect. Immun.* 76:1748–1755. http://dx.doi.org/10.1128/IAI.01333-07

Amanna, I.J., and M.K. Slifka. 2010. Mechanisms that determine plasma cell lifespan and the duration of humoral immunity. *Immunol. Rev.* 236:125–138. http://dx.doi.org/10.1111/j.1600-065X.2010.00912.x

Amanna, I.J., N.E. Carlson, and M.K. Slifka. 2007. Duration of humoral immunity to common viral and vaccine antigens. *N. Engl. J. Med.* 357:1903–1915. http://dx.doi.org/10.1056/NEJMoa066092

Bernasconi, N.L., E. Traggiai, and A. Lanzavecchia. 2002. Maintenance of serological memory by polyclonal activation of human memory B cells. *Science.* 298:2199–2202. http://dx.doi.org/10.1126/science.1076071

Bouharoun-Tayoun, H., P. Attanath, A. Sabchareon, T. Chongsuphajaisiddhi, and P. Druilhe. 1990. Antibodies that protect humans against *Plasmodium falciparum* blood stages do not on their own inhibit parasite growth and invasion in vitro, but act in cooperation with monocytes. *J. Exp. Med.* 172:1633–1641. http://dx.doi.org/10.1084/jem.172.6.1633

Cohen, S., I.A. McGREGOR, and S. Carrington. 1961. Gamma-globulin and acquired immunity to human malaria. *Nature.* 192:733–737. http://dx.doi.org/10.1038/192733a0

Courtin, D., M. Oesterholt, H. Huismans, K. Kusi, J. Milet, C. Badaut, O. Gaye, W. Roeffen, E.J. Remarque, R. Sauerwein, et al. 2009. The quantity and quality of African children's IgG responses to merozoite surface antigens reflect protection against Plasmodium falciparum malaria. *PLoS ONE.* 4:e7590. http://dx.doi.org/10.1371/journal.pone.0007590

Dal-Bianco, M.P., K.B. Köster, U.D. Kombila, J.F. Kun, M.P. Grobusch, G.M. Ngoma, P.B. Matsiegui, C. Supan, C.L. Salazar, M.A. Missinou, et al. 2007. High prevalence of asymptomatic Plasmodium falciparum infection in Gabonese adults. *Am. J. Trop. Med. Hyg.* 77:939–942.

de Stricker, K., J.Vuust, S. Jepsen, C. Oeuvray, and M.Theisen. 2000. Conservation and heterogeneity of the glutamate-rich protein (GLURP) among field isolates and laboratory lines of Plasmodium falciparum. *Mol. Biochem. Parasitol.* 111:123–130. http://dx.doi.org/10.1016/S0166-6851(00)00304-2

Dorfman, J.R., P. Bejon, F.M. Ndungu, J. Langhorne, M.M. Kortok, B.S. Lowe, T.W. Mwangi, T.N. Williams, and K. Marsh. 2005. B cell memory to 3 *Plasmodium falciparum* blood-stage antigens in a malaria-endemic area. *J. Infect. Dis.* 191:1623–1630. http://dx.doi.org/10.1086/429671

Ehrhardt, G.R., J.T. Hsu, L. Gartland, C.M. Leu, S. Zhang, R.S. Davis, and M.D. Cooper. 2005. Expression of the immunoregulatory molecule FcRH4 defines a distinctive tissue-based population of memory B cells. *J. Exp. Med.* 202:783–791. http://dx.doi.org/10.1084/jem.20050879

Ehrhardt, G.R., A. Hijikata, H. Kitamura, O. Ohara, J.Y. Wang, and M.D. Cooper. 2008. Discriminating gene expression profiles of memory B cell subpopulations. *J. Exp. Med.* 205:1807–1817. http://dx.doi.org/10.1084/jem.20072682

Esen, M., P.G. Kremsner, R. Schleucher, M. Gässler, E.B. Imoukhuede, N. Imbault, O. Leroy, S. Jepsen, B.W. Knudsen, M. Schumm, et al. 2009. Safety and immunogenicity of GMZ2 – a MSP3-GLURP fusion protein malaria vaccine candidate. *Vaccine.* 27:6862–6868. http://dx.doi.org/10.1016/j.vaccine.2009.09.011

Fowkes, F.J., J.S. Richards, J.A. Simpson, and J.G. Beeson. 2010. The relationship between anti-merozoite antibodies and incidence of *Plasmodium falciparum* malaria: A systematic review and meta-analysis. *PLoS Med.* 7:e1000218. http://dx.doi.org/10.1371/journal.pmed.1000218

Gardner, M.J., N. Hall, E. Fung, O. White, M. Berriman, R.W. Hyman, J.M. Carlton, A. Pain, K.E. Nelson, S. Bowman, et al. 2002. Genome sequence of the human malaria parasite *Plasmodium falciparum*. *Nature.* 419:498–511. http://dx.doi.org/10.1038/nature01097

Garnham, P.C. 1949. Malarial immunity in Africans; effects in infancy and early childhood. *Ann. Trop. Med. Parasitol.* 43:47–61.

Haynes, B.F., J. Fleming, E.W. St Clair, H. Katinger, G. Stiegler, R. Kunert, J. Robinson, R.M. Scearce, K. Plonk, H.F. Staats, et al. 2005. Cardiolipin polyspecific autoreactivity in two broadly neutralizing HIV-1 antibodies. *Science.* 308:1906–1908. http://dx.doi.org/10.1126/science.1111781

Johnson, J.D., R.A. Dennull, L. Gerena, M. Lopez-Sanchez, N.E. Roncal, and N.C. Waters. 2007. Assessment and continued validation of the malaria SYBR green I-based fluorescence assay for use in malaria drug screening. *Antimicrob. Agents Chemother.* 51:1926–1933. http://dx.doi.org/10.1128/AAC.01607-06

Langhorne, J., F.M. Ndungu, A.M. Sponaas, and K. Marsh. 2008. Immunity to malaria: more questions than answers. *Nat. Immunol.* 9:725–732. http://dx.doi.org/10.1038/ni.f.205

Lucumi, E., C. Darling, H. Jo, A.D. Napper, R. Chandramohanadas, N. Fisher, A.E. Shone, H.Jing, S.A.Ward, G.A. Biagini, et al. 2010. Discovery of potent small-molecule inhibitors of multidrug-resistant *Plasmodium falciparum* using a novel miniaturized high-throughput luciferase-based assay. *Antimicrob. Agents Chemother.* 54:3597–3604. http://dx.doi.org/10.1128/AAC.00431-10

Manske, M., O. Miotto, S. Campino, S. Auburn, J. Almagro-Garcia, G. Maslen, J. O'Brien, A. Djimde, O. Doumbo, I. Zongo, et al. 2012. Analysis of *Plasmodium falciparum* diversity in natural infections by deep sequencing. *Nature*. 487:375–379. http://dx.doi.org/10.1038/nature11174

Meffre, E., A. Schaefer, H. Wardemann, P. Wilson, E. Davis, and M.C. Nussenzweig. 2004. Surrogate light chain expressing human periph-eral B cells produce self-reactive antibodies. *J. Exp. Med*. 199:145–150. http://dx.doi.org/10.1084/jem.20031550

Meraldi, V., I. Nebié, A.B. Tiono, D. Diallo, E. Sanogo, M. Theisen, P. Druilhe, G. Corradin, R. Moret, and B.S. Sirima. 2004. Natural anti-body response to *Plasmodium falciparum* Exp-1, MSP-3 and GLURP long synthetic peptides and association with protection. *Parasite Immunol*. 26:265–272. http://dx.doi.org/10.1111/j.0141-9838.2004.00705.x

Moir, S., J. Ho, A. Malaspina, W. Wang, A.C. DiPoto, M.A. O'Shea, G. Roby, S. Kottilil, J. Arthos, M.A. Proschan, et al. 2008. Evidence for HIV-associated B cell exhaustion in a dysfunctional memory B cell compartment in HIV-infected viremic individuals. *J. Exp. Med*. 205:1797–1805. http://dx.doi.org/10.1084/jem.20072683

Moir, S., C.M. Buckner, J. Ho, W. Wang, J. Chen, A.J. Waldner, J.G. Posada, L. Kardava, M.A. O'Shea, S. Kottilil, et al. 2010. B cells in early and chronic HIV infection: evidence for preservation of immune function associated with early initiation of antiretroviral therapy. *Blood*. 116:5571–5579. http://dx.doi.org/10.1182/blood-2010-05-285528

Mouquet, H., and M.C. Nussenzweig. 2012. Polyreactive antibodies in adaptive immune responses to viruses. *Cell. Mol. Life Sci*. 69:1435–1445. http://dx.doi.org/10.1007/s00018-011-0872-6

Mouquet, H., J.F. Scheid, M.J. Zoller, M. Krogsgaard, R.G. Ott, S. Shukair, M.N. Artyomov, J. Pietzsch, M. Connors, F. Pereyra, et al. 2010. Polyreactivity increases the apparent affinity of anti-HIV antibodies by het-eroligation. *Nature*. 467:591–595. http://dx.doi.org/10.1038/nature09385

Murray, C.J., L.C. Rosenfeld, S.S. Lim, K.G. Andrews, K.J. Foreman, D. Haring, N. Fullman, M. Naghavi, R. Lozano, and A.D. Lopez. 2012. Global malaria mortality between 1980 and 2010: a systematic analysis. *Lancet*. 379:413–431. http://dx.doi.org/10.1016/S0140-6736(12)60034-8

Nduati, E.W., D.H. Ng, F.M. Ndungu, P. Gardner, B.C. Urban, and J. Langhorne. 2010. Distinct kinetics of memory B-cell and plasma-cell re-sponses in peripheral blood following a blood-stage *Plasmodium chabaudi* infection in mice. *PLoS ONE*. 5:e15007. http://dx.doi.org/10.1371/journal.pone.0015007

Ndungu, F.M., E.T. Cadman, J. Coulcher, E. Nduati, E. Couper, D.W. Macdonald, D. Ng, and J. Langhorne. 2009. Functional memory B cells and long-lived plasma cells are generated after a single *Plasmodium chabaudi* infection in mice. *PLoS Pathog*. 5:e1000690. http://dx.doi.org/10.1371/journal.ppat.1000690

Ndungu, F.M., A. Olotu, J. Mwacharo, M. Nyonda, J. Apfeld, L.K. Mramba, G.W. Fegan, P. Bejon, and K. Marsh. 2012. Memory B cells are a more reliable archive for historical antimalarial responses than plasma antibodies in no-longer exposed children. *Proc. Natl. Acad. Sci. USA*. 109:8247–8252. http://dx.doi.org/10.1073/pnas.1200472109

Nogaro, S.I., J.C. Hafalla, B. Walther, E.J. Remarque, K.K. Tetteh, D.J. Conway, E.M. Riley, and M. Walther. 2011. The breadth, but not the magnitude, of circulating memory B cell responses to P. falciparum increases with age/exposure in an area of low transmission. *PLoS ONE*. 6:e25582. http://dx.doi.org/10.1371/journal.pone.0025582

Reynaud, C.A., M. Descatoire, I. Dogan, F. Huetz, S. Weller, and J.C. Weill. 2012. IgM memory B cells: a mouse/human paradox. *Cell. Mol. Life Sci*. 69:1625–1634. http://dx.doi.org/10.1007/s00018-012-0971-z

Rodríguez, L.E., H. Curtidor, M. Ocampo, J. Garcia, A. Puentes, J. Valbuena, R. Vera, R. López, and M.E. Patarroyo. 2005. Identifying *Plasmodium falciparum* merozoite surface antigen 3 (MSP3) protein peptides that bind specifically to erythrocytes and inhibit merozoite invasion. *Protein Sci*. 14:1778–1786. http://dx.doi.org/10.1110/ps.041304505

Roestenberg, M., G.A. O'Hara, C.J. Duncan, J.E. Epstein, N.J. Edwards, A. Scholzen, A.J. van der Ven, C.C. Hermsen, A.V. Hill, and R.W.

Sauerwein. 2012. Comparison of clinical and parasitological data from controlled human malaria infection trials. *PLoS ONE*. 7:e38434. http://dx.doi.org/10.1371/journal.pone.0038434

Scheid, J.F., H. Mouquet, B. Ueberheide, R. Diskin, F. Klein, T.Y. Oliveira, J. Pietzsch, D. Fenyo, A. Abadir, K. Velinzon, et al. 2011. Sequence and structural convergence of broad and potent HIV anti-bodies that mimic CD4 binding. *Science*. 333:1633–1637. http://dx.doi.org/10.1126/science.1207227

Singh, S., S. Soe, S. Weisman, J.W. Barnwell, J.L. Pérignon, and P. Druilhe. 2009. A conserved multi-gene family induces cross-reactive antibodies effective in defense against *Plasmodium falciparum*. *PLoS ONE*. 4:e5410. http://dx.doi.org/10.1371/journal.pone.0005410

Smilkstein, M., N. Sriwilaijaroen, J.X. Kelly, P. Wilairat, and M. Riscoe. 2004. Simple and inexpensive fluorescence-based technique for high-through-put antimalarial drug screening. *Antimicrob. Agents Chemother*. 48:1803–1806. http://dx.doi.org/10.1128/AAC.48.5.1803-1806.2004

Struik, S.S., and E.M. Riley. 2004. Does malaria suffer from lack of memory? *Immunol. Rev*. 201:268–290. http://dx.doi.org/10.1111/j.0105-2896.2004.00181.x

Taylor, R.R., A. Egan, D. McGuinness, A. Jepson, R. Adair, C. Drakely, and E. Riley. 1996. Selective recognition of malaria antigens by human serum antibodies is not genetically determined but demonstrates some features of clonal imprinting. *Int. Immunol*. 8:905–915. http://dx.doi.org/10.1093/intimm/8.6.905

Theisen, M., S. Soe, K. Brunstedt, F. Follmann, L. Bredmose, H. Israelsen, S.M. Madsen, and P. Druilhe. 2004. A *Plasmodium falciparum* GLURP-MSP3 chimeric protein; expression in *Lactococus lactis*, immunogenicity and induction of biologically active antibodies. *Vaccine*. 22:1188–1198. http://dx.doi.org/10.1016/j.vaccine.2003.09.017

Tiller, T., E. Meffre, S. Yurasov, M. Tsuiji, M.C. Nussenzweig, and H. Wardemann. 2008. Efficient generation of monoclonal antibodies from single human B cells by single cell RT-PCR and expression vector cloning. *J. Immunol. Methods*. 329:112–124. http://dx.doi.org/10.1016/j.jim.2007.09.017

Tongren, J.E., C.J. Drakeley, S.L. McDonald, H.G. Reyburn, A. Manjurano, W.M. Nkya, M.M. Lemnge, C.D. Gowda, J.E. Todd, P.H. Corran, and E.M. Riley. 2006. Target antigen, age, and dura-tion of antigen exposure independently regulate immunoglobulin G subclass switching in malaria. *Infect. Immun*. 74:257–264. http://dx.doi.org/10.1128/IAI.74.1.257-264.2006

Wardemann, H., S. Yurasov, A. Schaefer, J.W. Young, E. Meffre, and M.C. Nussenzweig. 2003. Predominant autoantibody production by early human B cell precursors. *Science*. 301:1374–1377. http://dx.doi.org/10.1126/science.1086907

Weiss, G.E., P.D. Crompton, S. Li, L.A. Walsh, S. Moir, B. Traore, K. Kayentao, A. Ongoiba, O.K. Doumbo, and S.K. Pierce. 2009. Atypical memory B cells are greatly expanded in individuals living in a malaria-endemic area. *J. Immunol*. 183:2176–2182. http://dx.doi.org/10.4049/jimmunol.0901297

Weiss, G.E., B. Traore, K. Kayentao, A. Ongoiba, S. Doumbo, D. Doumtabe, Y. Kone, S. Dia, A. Guindo, A. Traore, et al. 2010. The *Plasmodium falciparum*-specific human memory B cell compartment expands gradu-ally with repeated malaria infections. *PLoS Pathog*. 6:e1000912. http://dx.doi.org/10.1371/journal.ppat.1000912

Weiss, G.E., E.H. Clark, S. Li, B. Traore, K. Kayentao, A. Ongoiba, J.N. Hernandez, O.K. Doumbo, S.K. Pierce, O.H. Branch, and P.D. Crompton. 2011. A positive correlation between atypical memory B cells and *Plasmodium falciparum* transmission intensity in cross-sectional studies in Peru and Mali. *PLoS ONE*. 6:e15983. http://dx.doi.org/10.1371/journal.pone.0015983

Wipasa, J., C. Suphavilai, L.C. Okell, J. Cook, P.H. Corran, K. Thaikla, W. Liewsaree, E.M. Riley, and J.C. Hafalla. 2010. Long-lived antibody and B Cell memory responses to the human malaria parasites, *Plasmodium falciparum* and *Plasmodium vivax*. *PLoS Pathog*. 6:e1000770. http://dx.doi.org/10.1371/journal.ppat.1000770